SO$_2$ adsorption on silica supported iridium

Djamela Bounechada,[a)] David P. Anderson, Magnus Skoglundh, and Per-Anders Carlsson[b)]
Department of Chemistry and Chemical Engineering and Competence Centre for Catalysis, Chalmers University of Technology, SE-412 96 Göteborg, Sweden

The interaction of SO$_2$ with Ir/SiO$_2$ was studied by simultaneous *in situ* diffuse reflectance infrared Fourier transform spectroscopy and mass spectrometry, exposing the sample to different SO$_2$ concentrations ranging from 10 to 50 ppm in the temperature interval 200–400 °C. Evidences of adsorption of sulfur species in both absence and presence of oxygen are found. For a pre-reduced sample in the absence of oxygen, SO$_2$ disproportionates such that the iridium surface is rapidly saturated with adsorbed S while minor amounts of formed SO$_3$ may adsorb on SiO$_2$. Adding oxygen to the feed leads to the oxidation of sulfide species that either (i) desorb as SO$_2$ and/or SO$_3$, (ii) remain at metal sites in the form of adsorbed SO$_2$, or (iii) spillover to the oxide support and form sulfates (SO$_4^{2-}$). Notably, significant formation of sulfates on silica is possible only in the presence of both SO$_2$ and O$_2$, suggesting that SO$_2$ oxidation to SO$_3$ is a necessary first step in the mechanism of formation of sulfates on silica. During the formation of sulfates, a concomitant removal/rearrangement of surface silanol groups is observed. Finally, the interaction of SO$_2$ with Ir/SiO$_2$ depends primarily on the temperature and type of gas components but only to a minor extent on the inlet SO$_2$ concentration. *Published by AIP Publishing.* [http://dx.doi.org/10.1063/1.4976835]

I. INTRODUCTION

Metal oxide supported iridium is used to catalyze a variety of chemical reactions including selective hydrogenation/dehydrogenation of hydrocarbons,[1–8] partial methane oxidation to syngas,[9] and reduction of nitric oxide.[10–12] The former two apply to chemical production while the latter finds relevance within the field of emission control. Nevertheless, in all cases it is often so that the catalyst becomes exposed towards sulfur species due to the presence of sulfur either as impurities in the process feedstock and/or solvent or contained in engine lubricants so that sulfur eventually ends up in downstream exhaust aftertreatment catalysts. The sulfur levels in the sources are usually low but even trace amounts may poison the catalytic functions,[13] which often leads to irreversible catalyst deactivation. In a few cases, however, the addition of sulfur has been found to, at least occasionally, promote catalytic reactions.[11,13–15] Supported iridium is an interesting type of material not only for catalytic processes but also for gas sensing technologies. For example, it can be used as a gate material for silicon carbide field-effect transistor (SiC-FET) devices.[16] Recently, SiC-FET sensors have been investigated for the detection of sulfur dioxide in desulfurization systems.[17,18]

To mechanistically clarify how sulfur dioxide poisons and promotes catalytic functions or impacts the response of a sensor device by interactions with the surface of the sensor, vibrational spectroscopic measurement of SO$_2$ adsorption under reaction conditions is one of the stronger methods available. Although widely used for *in situ* studies of a variety of supported noble metal catalysts,[13,14,19–21] it seems that the corresponding studies for silica supported Ir are still lacking. Among the few exceptions are the works by Haneda *et al.*[11] and Yoshinari *et al.*,[15] who showed that reduction of nitric oxide with carbon monoxide or hydrogen over an Ir/SiO$_2$ catalyst is possible only in the presence of both oxygen and sulfur dioxide. They suggested that SO$_2$ adsorbs strongly on Ir in the absence of oxygen inhibiting NO adsorption and its consecutive reduction. On the contrary, the presence of oxygen leads to the oxidation of SO$_2$ into SO$_3$ that upon desorption leaves vacant iridium sites for NO reduction. Unfortunately, their proposal could not be confirmed by infrared spectroscopic measurements due to the strong absorption of infrared radiation by the silica in the wavenumber region of interest for ad-SO$_x$ species.[15]

One possible strategy to overcome the spectroscopic complications imposed by the opacity of silica is to dilute the sample with a suitable diluent. In the case of analyzing powder samples using diffuse reflectance infrared Fourier transform spectroscopy (DRIFTS), highly reflecting alkali halides such as potassium bromide (KBr) or calcium fluoride (CaF$_2$) powders are often used as diluents. These compounds, however, may react with the introduced gases causing undesired IR absorption bands overlaying the absorption bands of interest related to the sample, which complicates the results' analysis. In worst case, the diluent material impacts the catalytic reactions or surface processes to be studied thereby causing artifactual results. Recently we showed that the use of diamond powder as diluent effectively increases the sample reflectance while only minor (weak) absorption bands are introduced.[22] In particular, we combined *in situ* DRIFTS and first-principles calculations to investigate how SO$_2$ interacts with the surface of Pt/SiO$_2$ representing a gas sensor model system.

[a)]Present address: Johnson Matthey Technology Centre, Blount's Court, Sonning Common, Reading RG4 9NH, UK.
[b)]Electronic address: per-anders.carlsson@chalmers.se

In the present work, we employ *in situ* DRIFTS and mass spectrometry (MS) to study the adsorption of SO_2 on Ir/SiO_2 both in the absence and presence of oxygen. Although the primary aim is to clarify the role played by the noble metal in the sensing mechanism of SO_2 on SiC-FET devices, the results presented here can in a general context be used also when encountering interaction of sulfur with Ir/SiO_2 catalysts.

II. EXPERIMENTAL SECTION

A. Sample preparation and characterisation

Colloidal silica (Kromasil Silica KR-300-10, Akzo Nobel Eka Chemicals) was instantly frozen with liquid nitrogen, freeze-dried, and thermally treated in air at 600 °C for 2 h. The 4 wt. % Ir/SiO_2 sample was prepared according to the wet-impregnation technique by dispersing the calcined silica sample in an aqueous solution of ammonium hexachloroiridate ($(NH_4)_2IrCl_6$, Sigma-Aldrich). After one hour of stirring, the sample was frozen by immersing the sample container in liquid nitrogen and subsequently freeze-dried. The dry sample was then calcined in air at 450 °C for 1 h using a heating rate of 5°/min from room temperature, in order to promote a high iridium dispersion.[23] During the calcination procedure, the sample changed color from purple to dark grey.

The parent sample was characterised with transmission electron microscopy using an FEI Tecnai G^2 T20 microscope with LaB_6 filament at 200 kV. A small amount of sample was dispersed in methanol using ultrasonication for about 20 s. One drop of the suspension was then placed onto a holey carbon Cu-grid with mesh 300 and subsequently dried for 30 min in air. Around 20 images were recorded at different magnifications. Furthermore X-ray photoelectron spectra of the Ir 4f region were recorded using a Quantum 2000 scanning ESCA microprobe with monochromatic Al Kα radiation at 1486.6 eV. The photoemission peak positions were charge corrected to the adventitious carbon signal at 284.8 eV.

B. *In situ* infrared spectroscopic equipment

A detailed description of the experimental setup used for the *in situ* DRIFTS-MS experiments can be found elsewhere.[22] Here we just briefly mention that a high-temperature stainless steel reaction cell (Harrick Scientific) coated with a silicon-based (Silcolloy 1000, SilcoTek) layer to improve its corrosion resistance in acidic environments and provided with KBr windows was used. Gases were introduced by individual mass flow controllers (Bronkhorst Low-ΔP-Flow). The feed of O_2 was carefully introduced by an air-actuated high-speed gas valve (Valco, VICI) in order to provide precise transients. The outlet gas composition was analyzed by mass spectrometry (Balzers QuadStar 420) following the mass-to-charge ratio (m/z): 2 (H_2), 18 (H_2O), 28 (CO), 32 (O_2 and S), 33 (HS), 34 (H_2S), 40 (Ar), 44 (CO_2), 48 (SO), 64 (SO_2), 80 (SO_3), 81 (SO_3), 82 (SO_3), and 83 (SO_3).

C. Experimental procedures

Before loading the sample into the reaction chamber the 4% Ir/SiO_2 sample was pressed into tablets, grounded in an agate mortar, and sieved as to single out grains with sizes between 40 and 100 μm. These grains were then mixed with natural diamond powder (40-60 μm, Alfa Aesar GmbH & Co KG) using a sample-to-diamond weight-ratio of 1:4. The diluted sample was then used for the DRIFT experiments.

For each experiment the sample was pretreated first by oxidation in 10 vol. % O_2 in Ar for 10 min and then by reduction in 4 vol. % H_2 in Ar at 400 °C for 10 min using a total flow of 100 ml/min. The sample was thereafter cooled in Ar with a rate of 10 °C/min until the temperature to be studied was reached, i.e., 200, 300, or 400 °C. The isothermal experiment was started, after 20 min dwelling in Ar, by feeding SO_2 for 15 min and then instantly adding 10 vol. % O_2 to the feed for another 15 min. Three different SO_2 levels, i.e., 10, 30, or 50 vol.-ppm were investigated independently at each temperature. Finally, after each experiment, the sample was regenerated with 4 vol.-% H_2 in Ar at 400 °C for 10 min.

The reference spectrum used for the background subtraction was collected 10 min before the introduction of SO_2 to the feed. Sample spectra were then collected every 30 s starting 2 min before the introduction of SO_2. The wavenumber region 1000-4000 cm^{-1} was investigated with a spectral resolution of 1 cm^{-1}.

III. RESULTS

Before describing the main *in situ* infrared spectroscopic results we comment on the characteristics of the as prepared sample. The TEM images in Figures 1(a) and 1(b) clearly show that the primary silica particles are around 30 nm in
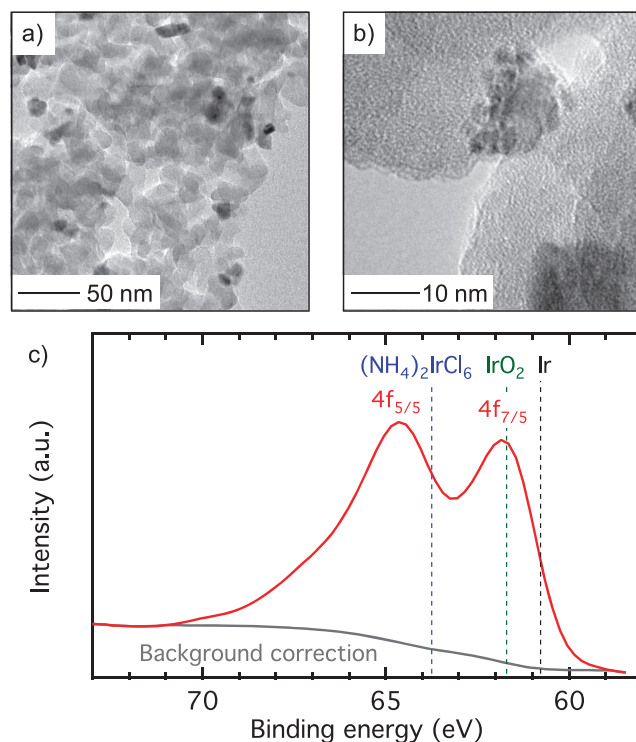

FIG. 1. Characterisation of the as prepared Ir/SiO_2 sample with TEM imaging (panels (a) and (b)) and high-resolution XPS of the Ir 4f region using Shirley background correction. The vertical dashed lines indicate the position of the $4f_{7/5}$ peaks for Ir, IrO_2, and $(NH_4)_2IrCl_6$ at 60.8, 61.6, and 63.7 eV, respectively.

diameter, in line with the specification by the supplier of the silica starting material. Concerning the iridium phase, which appears as dark regions, the vast majority of the iridium particles are below 1 nm while (very) few are bigger, around 10 nm. The small particles are often concentrated to certain regions and seem nearly agglomerated, which leads to visible dark areas in the size of 10-20 nm. The large proportion of small particles agrees well with the fact that the calcination procedure used here was similar to the one used by Shibuya *et al.* developed as to promote high dispersion of iridium when silica is used as a support.[23] The change in color from purple to dark grey during calcination reflects that the adsorbed iridium precursor complex has decomposed and formed small iridium particles. The high-resolution XPS measurements of the Ir 4f region, i.e., $4f_{5/2}$ and $4f_{7/5}$ peaks, are displayed in Figure 1(c). The vertical dashed lines indicate the $4f_{7/5}$ peak for the Ir, IrO_2, and $(NH_4)_2IrCl_6$ at 60.8, 61.6, and 63.7 eV, respectively. It is clear that no iridium complex remains on the surface after calcination. Instead a well pronounced signal for oxidised iridium is seen, reflecting that the iridium particles are (surface) oxidised.[24] This is expected as the sample was calcined in air.

Figures 2(a)–2(c) show the IR absorption spectra collected for Ir/SiO_2 sample pretreated at 200, 300, and 400 °C prior to the SO_2 exposure experiment. The spectra, which are used for background subtraction, overlap fairly well suggesting that each SO_2 exposure experiment starts from a common initial surface composition. Despite the sample dilution with diamond, almost complete absorption of the IR radiation is observed below 1200 cm^{-1}. Thus the region between 1200 and 1000 cm^{-1} is omitted in the following description of the results.

Figure 3 shows the evolution of absorption bands (difference spectra) in the wavenumber regions 1200-1900 and 2600-4000 cm^{-1} during exposure to SO_2 and $SO_2 + O_2$ at 200, 300, and 400 °C. At the lower temperatures (200 and 300 °C) significant changes are difficult to discern except for the region above 3800 cm^{-1} during $SO_2 + O_2$ exposure at 300 °C. Some minor absorption bands occur, which will be shown and discussed in more detail below. On the contrary, during $SO_2 + O_2$ exposure at 400 °C, a clear absorption band appears at 1300-1380 cm^{-1} and several bands occur in the wavenumber regions 3100-3400 and 3800-4000 cm^{-1}. Although these images appropriately show the dynamics of the growing absorption bands, it is easier to make assignments using the two-dimensional representation of the data as shown in Figures 4(a)–4(c). Here the difference IR spectra for the SO_2 exposure experiments at 200, 300, and 400 °C collected after 15 min of exposure of the sample to 10, 30, and 50 ppm of SO_2 and after another 15 min of exposure to the same concentrations of SO_2 in the presence of 10% O_2 are shown. The absorption band between 1300 and 1380 cm^{-1} is assigned to SO_2 adsorbed on iridium. Further, the absorption bands at 1380–1480 cm^{-1} and 3400–3900 cm^{-1} are assigned to sulfates on silica and terminal silanols, respectively. Schemes of these surface species and assignments have been presented previously.[22] Figures 5(a), 5(d), and 5(g) show the evolution (integrated peak area) of SO_2 adsorbed on iridium while Figures 5(b), 5(e), and 5(h) show the evolution of sulfates on silica and terminal silanols.
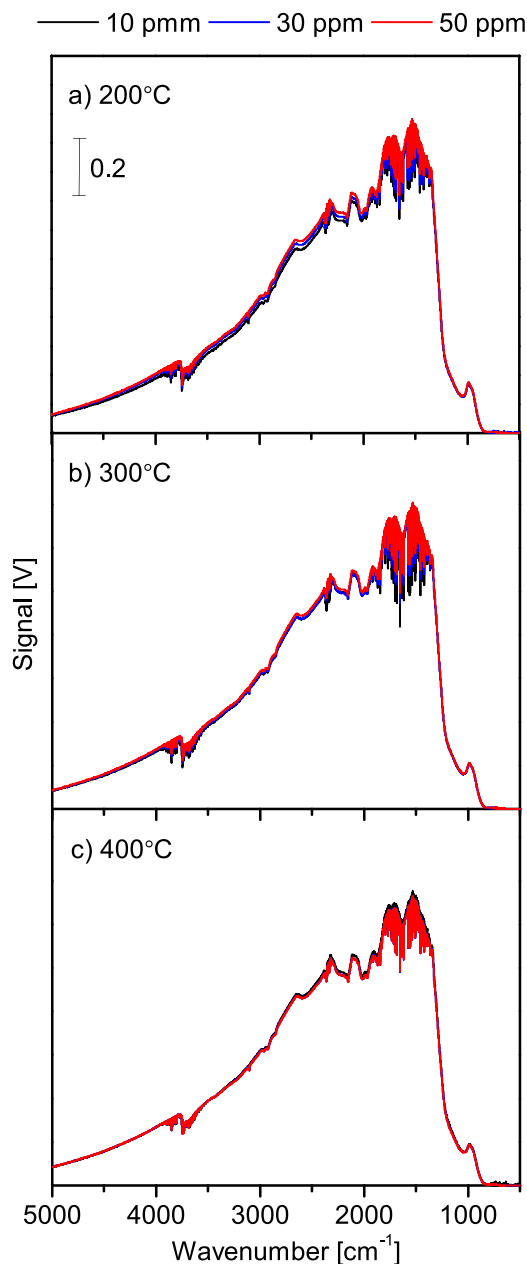

FIG. 2. IR absorption spectra of Ir/SiO_2 pretreated at (a) 200 °C, (b) 300 °C, and (c) 400 °C in Ar flow (100 ml/min) before the exposure to 10, 30, and 50 ppm of SO_2.

Since the results are both qualitatively and quantitatively similar for the different SO_2 exposures, we describe the spectral features together hereunder.

Introduction of SO_2 to the reduced sample (cf. Figure 4) does not result in changes in the IR spectra for the temperatures studied. The intensity of the absorption band for SO_2 adsorbed on iridium remains constant and close to zero during the entire period (cf. Figure 5). On the contrary, when O_2 is added to the feed several absorption bands occur. At 200 °C a band at 1344 cm^{-1} appears, which is due to SO_2 adsorbed on Ir. The evolution of this band increases sharply upon the introduction of oxygen (cf. Figure 5(a)). The areas of the absorption bands related to sulfates on silica and terminal silanols (cf. Figure 5(b)) remain fairly constant and close to zero during the experiments. It is worth to note that
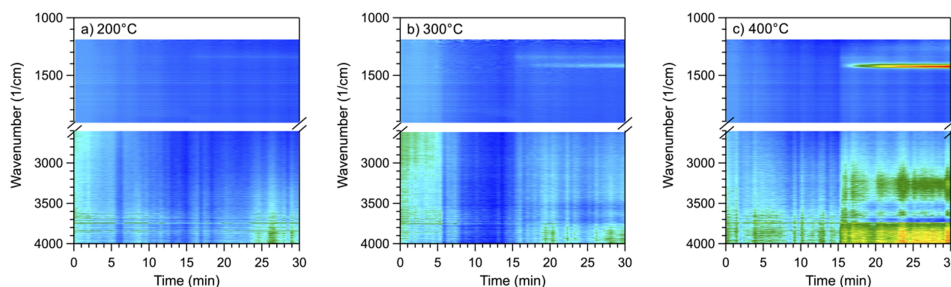
FIG. 3. Exposure of 50 ppm SO_2 (t = 0-15 min) and 50 ppm SO_2 + 10% O_2 (t = 15-30 min) to Ir/SiO$_2$ at (a) 200, (b) 300, and (c) 400 °C. The panels show the color coded intensities, where red corresponds to high intensity (individual color code for each panel), of the IR bands (log 1/R, arbitrary units) in the regions 1200-1900 and 2600-4000 cm^{-1} versus time.

a clear increase of the SO_2 outlet concentration for about three minutes after introduction of the oxygen is observed (cf. Figure 5(c)), followed by a decrease for about 2 min and then an increase.

The results of the SO_2 exposure experiments performed at 300 °C are shown in Figure 4(b). Similar to the experiment at 200 °C, no significant changes occur in the absence of oxygen. As soon as oxygen is added to the feed, the absorption band at 1350 cm^{-1}, related to SO_2 adsorbed on Ir, appears. In contrast to the experiment performed at lower temperature, the introduction of oxygen gives rise to a new absorption band at 1420 cm^{-1}, which is the characteristic of sulfate species adsorbed on silica,[25] and two negative bands in the silanol region, i.e., at 3727 and 3525 cm^{-1}, which are assigned to isolated[26,27] and vicinal (H-bonded)[26,28] silanols (SiOH), respectively. The spectral features described so far are common for all SO_2 feed concentrations. The intensities of the absorption bands attributed to sulfates on silica and silanols increase with increasing SO_2 concentration. In all cases the integrated area of the absorption band related to adsorbed SO_2 remains close to zero when only SO_2 is fed and then increases stepwise at the oxygen switch and remains during the following 15 min (cf. Figure 5(d)). The areas of the absorption bands of sulfates on silica and silanols remain constant and close to zero during the first 15 min of SO_2 exposure. Then, in the presence of oxygen, the intensity of these bands increases/decreases almost linearly, respectively (cf. Figure 5(e)). The MS measurements show a sharp increase in the SO_2 outlet concentration for about 3, 1.5, and 1 min after the oxygen switch during the experiments performed with 10, 30, and 50 ppm SO_2, respectively (cf. Figure 5(f)). The SO_2 concentration then decreases for 2, 3.5, and 5 min, respectively, before increasing again in the case of 30 and 50 ppm of inlet SO_2 and remains constant and close to zero in the case of 10 ppm of inlet SO_2.

For the experiment carried out at 400 °C (cf. Figure 4(c)), no absorption bands are detected during the exposure to SO_2 in the absence of oxygen. When oxygen is introduced to the feed a positive absorption band related to sulfates on silica appears at 1425 cm^{-1}, which is accompanied by two negative bands at 3724 and 3549 cm^{-1} corresponding to isolated and vicinal silanols, respectively. Furthermore, four new positive absorption bands become visible at 3744, 3262, 3106, and 1262 cm^{-1} in the case of 30 and 50 ppm SO_2 and oxygen. The sharp band at 3744 cm^{-1} can be assigned to geminal silanols,[29]

whereas the broader bands at 3262 and 3106 cm^{-1} previously have been assigned to perturbed silanols (H-bonded with sulfates adsorbed on silica) or C–H stretching mode of diamond species.[30,31] Finally, although not very clear, the
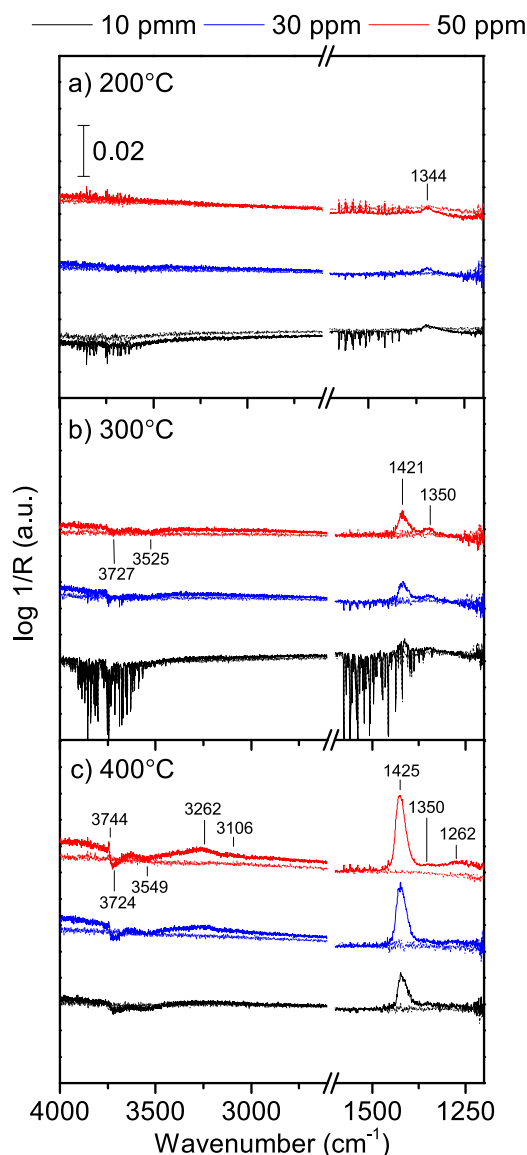

FIG. 4. Difference IR absorption spectra of Ir/SiO$_2$ collected at (a) 200 °C, (b) 300 °C, and (c) 400 °C after 15 min of exposure to SO_2 (dotted lines) and after further 15 min of exposure to SO_2 in the presence of 10% O_2 (solid lines) (100 ml/min of total flow).
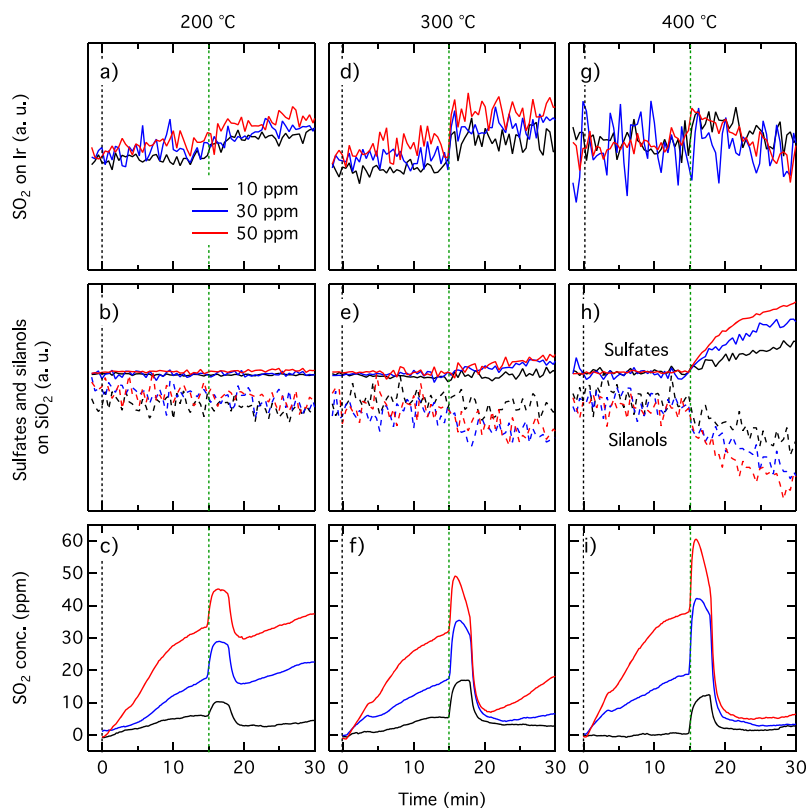
FIG. 5. Integrated peak areas of SO_2 (between 1300 and 1380 cm^{-1}) adsorbed on Ir (top panels) and sulfates on silica (between 1380 and 1480 cm^{-1}) and terminal silanols (between 3400 and 3900 cm^{-1}) (middle panels) for the experiments at (a) 200 °C, (b) 300 °C, and (c) 400 °C. Outlet SO_2 concentration profiles detected during the exposure of Ir/SiO$_2$ to SO_2 (bottom panels). The vertical dashed line indicates the introduction of SO_2 (black) and addition of O$_2$ (green), respectively.

appearance of an absorption band at 1350 cm^{-1} due to SO_2 adsorbed on Ir cannot be excluded. The areas related to sulfates adsorbed on silica and silanols remain close to zero during the first 15 min of SO_2 exposure. Then, during the following 15 min in the presence of oxygen, these bands increase and decrease, respectively. The intensity of the bands increases with increased inlet SO_2 concentration (cf. Figure 5(h)). The outlet concentrations of SO_2 are in large qualitatively similar to those observed at 300 °C with the only exception that the increase of SO_2 concentration towards the end of the experiments is significantly lower (cf. Figure 5(i)). Finally, an attempt to quantification is shown in Figure 6, where the IR absorption spectra during the exposure of the sample to different inlet concentrations but the same total amount (0.67 μmol) of SO_2 are directly compared. The spectra collected at the same temperature with different inlet SO_2 concentrations are fairly overlapped.

IV. DISCUSSION

The catalytic oxidation of SO_2 to SO_3 has been studied for many technological systems as it presents an important reaction in a variety of applications.[32–35] Here, the adsorption of SO_2 on Ir/SiO$_2$ presents undoubtable similarities with the corresponding experiments with Pt/SiO$_2$.[22] For example, the formation of sulfates on silica occurs with a concomitant removal/rearrangement of silanols (cf. Figures 4, 5(b), 5(e), and 5(h)). The absorption band related to sulfates on silica at about 1420 cm^{-1} was detected only in the presence of oxygen, suggesting that SO_2 oxidation to SO_3 over the iridium is a crucial first step in the sulfate formation process. Likely, due to the

different activity to oxidize SO_2 of platinum and iridium, the formation of sulfate species on silica occurs already at 200 °C on the Pt/SiO$_2$ sample, whereas temperatures between 200 and 300 °C are required to promote the formation of sulfates on the Ir/SiO$_2$ sample. Interestingly, however, there are also some remarkable differences between the Ir/SiO$_2$ and Pt/SiO$_2$ samples.

The first difference compared to the Pt/SiO$_2$ system is the significant temporary increase in the outlet SO_2 concentration upon the introduction of oxygen as seen for all temperatures (cf. Figures 5(c), 5(f), and 5(i)). This indicates a release of a substantial amount of ad-SO$_x$ species that have
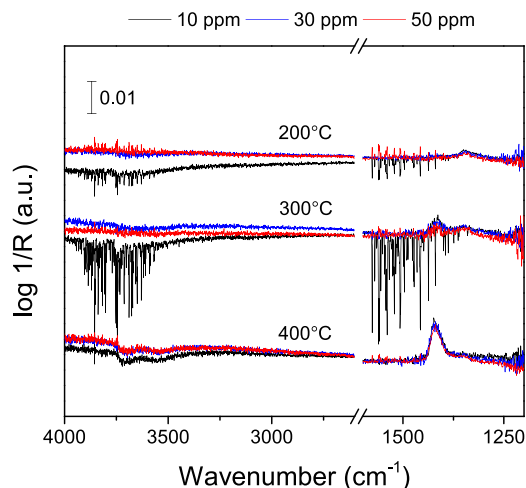

FIG. 6. Difference IR absorption spectra collected at 200, 300, and 400 °C after exposure of Ir/SiO$_2$ to the same amount of SO_2 (0.67 μmol) in the presence of O$_2$.

been accumulated on the iridium surface during the oxygen-free period. As for this period no significant changes in the IR spectra could be observed, these species are likely to be inactive for IR absorption. This suggests the formation of sulfides in the absence of oxygen, as adsorbed S cannot be probed with IR spectroscopy. It has been shown for extended surfaces of iridium that adsorbed SO is an intermediate when SO_2 disproportionates into atomic sulfur and SO_3 through disproportionation.[36] Depending on temperature SO_3 may remain adsorbed ($<130\,°C$) or desorb ($>230\,°C$) leaving adsorbed S on the surface.[36] From the present results under oxygen-free conditions, one may envisage that SO_2 is reduced to form both SO and S species on the Ir surface. The wavenumber for IR absorption by free SO molecules has been shown by isotope labelling experiments to be $1137\ cm^{-1}$.[37] In the present experiments no such absorption bands could be observed (not shown). The SO species, however, is expected to be short-lived when adsorbed on the Ir surface and would immediately dissociate further to adsorbed S and O.[38] Similar arguments have been put forward for the stability of SO on Pd based on X-ray photoelectron measurements and first-principles calculations.[33] The adsorbed oxygen may react with adsorbing SO_2 until the surface is completely covered with S and further SO_2 dissociation is inhibited.

The second difference is the absorption band that appears at $1350\ cm^{-1}$ when oxygen is introduced to the feed (cf. Figures 4, 5(a), 5(d), and 5(g)). As soon as oxygen is introduced, the sulfur species adsorbed can be oxidized to SO_2 (and/or SO_3), which can remain on the surface of the sample in the form of SO_2 adsorbed on iridium ($1350\ cm^{-1}$), spillover to the silica support and form sulfates (SO_4^{2-}, $1420\ cm^{-1}$), or alternatively desorb to the gas phase, giving rise to a peak in the outlet SO_2 concentration.

Finally, the IR spectra collected after the exposure of the sample to the same amount of SO_2 ($0.67\ \mu mol$) but for different inlet SO_2 concentrations (10, 30, and 50 ppm) overlap at all the temperatures investigated. This potentially means that it would be difficult to distinguish between different SO_2 concentrations when using Ir as a gate material for SiC-FET sensors.

In summary we envisage that for oxygen-free conditions SO_2 disproportionates on iridium forming as an intermediate SO that rapidly dissociates further to adsorbed S and O. Adsorbed O then reacts further with adsorbed SO_2 to SO_3, which may adsorb on the silica surface. The iridium surface, however, rapidly becomes covered by S and the SO_2 disproportionation declines. This leads to minor amounts of sulfur being adsorbed on silica under oxygen-free conditions. In the presence of oxygen, adsorbed S and SO_2 are oxidised to SO_3, which leads to higher amount of sulfur adsorbed on silica. Under these conditions, iridium oxide is likely formed, which may explain the somewhat reduced signal-to-noise ratio when oxygen is introduced to the feed.

V. CONCLUSIONS

In the present work we have studied how SO_2 interacts with a pre-reduced Ir/SiO_2 sample by *in situ* DRIFT spectroscopy. We found that in the absence of oxygen SO_2 can

be adsorbed as sulfide on Ir and possibly, but not likely, as SO. The sulfide formation is likely to occur through a SO_2 disproportionation process where adsorbed SO is a short-lived species. When O_2 becomes available in the feed, the adsorbed reduced species can be oxidized and follow three possible routes: (i) desorb as SO_2 (or SO_3) to the gas phase, (ii) remain adsorbed as SO_2 on iridium, or (iii) spillover to the silica support, where sulfates (SO_4^{2-}) are formed. The presence of oxygen is a prerequisite for sulfate formation on silica, which suggests that SO_2 oxidation to SO_3 is the first step (after adsorption of SO_2 and O_2) in the sulfate formation mechanism. Comparison with the results of a previous study on SO_2 adsorption on Pt/SiO_2 allows the conclusion that the operating temperature range of SiC-FET devices for SO_2 detection and their sensitivity to atmospheres where O_2 is present can be modulated by changing the metal used at the gate.

[1] S. Nishimura, *Handbook of Heterogeneous Catalytic Hydrogenation for Organic Synthesis* (John Wiley & Sons, Inc., 2001).

[2] P. Mäki-Arvela, J. Hajek, T. Salmi, and D. Y. Murzin, Appl. Catal., A **292**, 1 (2005).

[3] P. Gallezot and D. Richard, Catal. Rev.: Sci. Eng. **40**, 81 (1998).

[4] E. N. Bakhanova, A. S. Astakhova, K. A. Brikenshtein, V. G. Dorokhov, V. I. Savchenko, and M. L. Khidekel', Russ. Chem. Bull. **21**(9), 1934 (1972).

[5] J. P. Breen, R. Burch, J. Gomez-Lopeza, K. Griffin, and M. Hayes, Appl. Catal., A **268**, 267 (2004).

[6] P. Reyes, M. C. Aguirre, I. Melián-Cabrera, M. L. Granados, and J. L. G. Fierro, J. Catal. **208**, 229 (2002).

[7] R. Frety, P. N. D. Silva, and M. Guenin, Catal. Lett. **3**, 9 (1989).

[8] P. Marecot, J. R. Mahoungou, and J. Barbier, Appl. Catal., A **101**, 143 (1993).

[9] K. Nakagawa, N. Ikenaga, T. Suzuki, T. Kobayashi, and M. Haruta, Appl. Catal., A **169**, 281 (1998).

[10] E. Iojoiu, P. Gélin, H. Praliaud, and M. Primet, Appl. Catal., A **263**, 39 (2004).

[11] M. Haneda, Pusparatu, Y. Kintaichi, I. Nakamura, M. Sasaki, T. Fujitani, and H. Hamada, J. Catal. **229**, 197 (2005).

[12] H. Inomata, M. Shimokawabe, A. Kuwan, and M. Arai, Appl. Catal., B **84**, 783 (2008).

[13] D. Bounechada, S. Fouladvand, L. Kylhammar, T. Pingel, E. Olsson, M. Skoglundh, J. Gustafson, M. D. Michiel, M. A. Newton, and P.-A. Carlsson, Phys. Chem. Chem. Phys. **15**, 8648 (2013).

[14] L. Kylhammar, P.-A. Carlsson, and M. Skoglundh, J. Catal. **284**, 50 (2011).

[15] T. Yoshinari, K. Sato, M. Haneda, Y. Kintaichi, and H. Hamada, Appl. Catal., B **41**, 157 (2003).

[16] M. Andersson, P. Ljung, M. Mattsson, M. Löfdahl, and A. L. Spetz, Top. Catal. **30/31**, 365 (2004).

[17] Z. Darmastuti, C. Bur, N. Lindqvist, and M. Anderson, Sens. Actuators, B **206**, 609 (2015).

[18] Z. Darmastuti, C. Bur, P. Möller, R. Rahlin, N. Lindqvist, M. Andersson, A. Schütze, and A. L. Spetz, Sens. Actuators, B **194**, 511 (2014).

[19] L. Kylhammar, P.-A. Carlsson, H. H. Ingelsten, H. Grönbeck, and M. Skoglundh, Appl. Catal., B **84**, 268 (2008).

[20] T. Luo and R. Gorte, Appl. Catal., B **53**, 77 (2004).

[21] J. A. Anderson, Z. Liua, and M. F. Garca, Catal. Today **113**, 25 (2006).

[22] D. Bounechada, Z. Darmastuti, M. Andersson, L. Ojamäe, A. L. Spetz, M. Skoglundh, and P.-A. Carlsson, J. Phys. Chem. C **118**, 29713 (2014).

[23] R. Shibuya, M.-A. Ohshima, H. Kurokawa, and H. Miural, Bull. Chem. Soc. Jpn. **83**, 732 (2010).

[24] V. Pfeifer, T. E. Jones, J. J. V. Vélez, C. Massué, M. T. Greiner, R. Arrigo, D. Teschner, F. Girgsdies, M. Scherzer, J. Allan *et al.*, Phys. Chem. Chem. Phys. **18**, 2292 (2116).

[25] B. G. Anderson, Z. Dang, and B. A. Morrow, J. Phys. Chem. **99**, 14444 (1995).

[26] B. A. Morrow and A. J. McFarlan, Langmuir **7**, 1695 (1991).

[27] G. Busca, Phys. Chem. Chem. Phys. **1**, 723 (1999).

[28] J. P. Gallas, J. M. Goupil, A. Vimont, J. C. Lavalley, B. Gil, J. P. Gilson, and O. Miserque, Langmuir **25**, 5825 (2009).

[29] Y. Iwasawa, *Tailored Metal Catalysts* (D. Riedel, Dordrecht, Holland, 1986).

[30] R. M. Silverstein, G. C. Bassler, and T. C. Morrill, *Spectrometric Identification of Organic Compounds*, 4th ed. (Wiley, Singapore, 1981).

[31] L. J. Hoyos, H. Praliaud, and M. Primet, Appl. Catal., A **98**, 125 (1993).

[32] S. Koutsopoulus, S. B. Rasmussen, K. M. Eriksen, and R. Fehrmann, Appl. Catal., B **306**, 142 (2006).

[33] K. Gotterbarm, N. Luckas, O. Höfert, M. A. Lorenz, R. Streber, C. Papp, F. Viñes, H.-P. Steinrück, and A. Görling, J. Chem. Phys. **136**, 094702 (2012).

[34] W. Benzinger, A. Wenka, and R. Dittmeyer, Appl. Catal., A **397**, 209 (2011).

[35] E. Xue, K. Seshan, and J. R. H. Ross, Appl. Catal., B **11**, 65 (1996).

[36] T. Fujitani, I. Nakamura, Y. Kobayashi, A. Takahashi, M. Haneda, and H. Hamada, Surf. Sci. **601**, 1615 (2007).

[37] A. G. Hopkins and C. W. Brown, J. Chem. Phys. **62**, 2511 (1975).

[38] R. Jiang, W. Guo, M. Li, H. Zhu, J. Li, L. Zhao, and D. F. H. Shan, J. Phys. Chem. C **113**, 18223 (2009).